Ocean Modelling 33 (2010) 20–32

Contents lists available at ScienceDirect

Ocean Modelling

journal homepage: www.elsevier.com/locate/ocemod

Gulf of California response to Hurricane Juliette

Luis Zamudio [a,*], E. Joseph Metzger [b], Patrick J. Hogan [b]

[a] Center for Ocean-Atmospheric Prediction Studies, Florida State University, Tallahassee, FL 32306-2840, USA
[b] Naval Research Laboratory, Stennis Space Center, MS, USA

ARTICLE INFO

Article history:
Received 1 August 2008
Received in revised form 16 November 2009
Accepted 21 November 2009
Available online 21 December 2009

Keyword:
Hurricane-generated coastal upwelling

ABSTRACT

The HYbrid Coordinate Ocean Model (HYCOM) has been configured for the Gulf of California (GOC) at 1/12° and 1/25° horizontal grid resolution and has been nested inside a basin-scale 1/12° Pacific version of HYCOM. The nested GOC models are used to study the upper-ocean GOC response to Hurricane Juliette. The model results indicate that Juliette's winds forced strong poleward coastal baroclinic currents (meridional velocity >60 cm/s) along the southwestern coast of the GOC. That reversed the well-observed mean equatorward currents along the southeastern coast of the Baja California Peninsula. These Juliette-induced currents forced a transport variation of >0.2 Sv along the entrance of the GOC. In addition, Juliette's winds increased the mixed layer depth (from ~5 m to ~40 m) and induced strong upwelling (vertical velocity >30 m/day) along the southeastern coast of the Baja California Peninsula. The model simulated upwelling is corroborated by model independent analysis of SeaWiFS chlorophyll-a satellite measurements. During its early stage Juliette generated a coastally trapped wave (CTW) along mainland Mexico. After its generation the CTW propagated poleward along the coasts of the mainland and GOC, where it reached the shelf break between the 28°N and 29°N and it reversed the direction and propagated equatorward along the western coast of the GOC. Next, the CTW propagated to the southwestern coast of the GOC, where it partially modulated the intensity of the Juliette-generated coastal upwelling.

1. Introduction

"The eastern tropical Pacific area of cyclone formation is relatively small compared with other cyclogenetic regions, but it accounts for nearly 17% of the global total of tropical storm development, with an average value of 14 storms per year (Hastenrath, 1991)" (Amador et al., 2006). Hence the eastern tropical Pacific area of generation of tropical cyclones is one of the most prolific regions of the planet, however, so far as we are aware, only five articles (Christensen et al., 1983; Enfield and Allen, 1983; Merrifield, 1992; Gjevik and Merrifield, 1993; Zamudio et al., 2002) have investigated some of the oceanographic processes generated by the passage of the tropical cyclones on the eastern Pacific. These valuable articles have mainly concentrated on the study of the evolution of coastal waves generated by the tropical cyclones.

On September 25, 2001 Hurricane Juliette sea-level pressure dropped to 923 mb. That is the second lowest measured sea-level pressure on record in the northeastern tropical Pacific Ocean. Associated with that low pressure, Juliette's winds intensified to 64 m/s and Juliette was upgraded to category 4 hurricane on the Saffir-Simpson Hurricane scale (http://www.nhc.noaa.gov). In general, Juliette followed an offshore pathway approximately parallel to the west coast of Mexico (Fig. 1a) and Juliette's winds generated a coastally trapped wave (CTW) between Acapulco and Manzanillo and lowered the sea surface temperature ~5 °C (Zamudio et al., 2002). During its path Hurricane Juliette neared the entrance of the Gulf of California generating significant variability on the circulation and volume transport, and forcing coastal upwellings. Hence, using the HYbrid Coordinate Ocean Model (HYCOM) as the main research tool, the present study documents some of the oceanographic processes generated by Hurricane Juliette around the southern end of the Gulf of California (GOC).

Since HYCOM is becoming a community model, the publicly accessible (http://www.hycom.org/dataserver) daily output of pre-operational global HYCOM can be used as boundary conditions for regional models. The coupling of global (or basin scale) to regional HYCOM is a one-way (from the outer grid to the inner grid) robust routine, which has been documented by Bleck et al. (2001) and Halliwell et al. (2009). This HYCOM to HYCOM coupling routine has been used to isolate dynamical processes at relatively low computational cost (Prasad and Hogan, 2007; Zamudio and Hogan, 2008; Zamudio et al., 2008; Kourafalou et al., 2009; Halliwell et al., 2009; Gierach et al., 2009) and has been extended to nest the Regional Ocean Model System (ROMS) into Atlantic and Global HYCOM. It has also been used in process studies along the West Florida Shelf (Barth et al. (2008a,2008b,2008c)) and the Philippine Archipelago (Han et al., 2009). Thus, the present study

* Corresponding author.
E-mail address: Luis.Zamudio.ctr.mx@nrlssc.navy.mil (L. Zamudio).

1463-5003/$ - see front matter © 2009 Elsevier Ltd. All rights reserved.
doi:10.1016/j.ocemod.2009.11.005

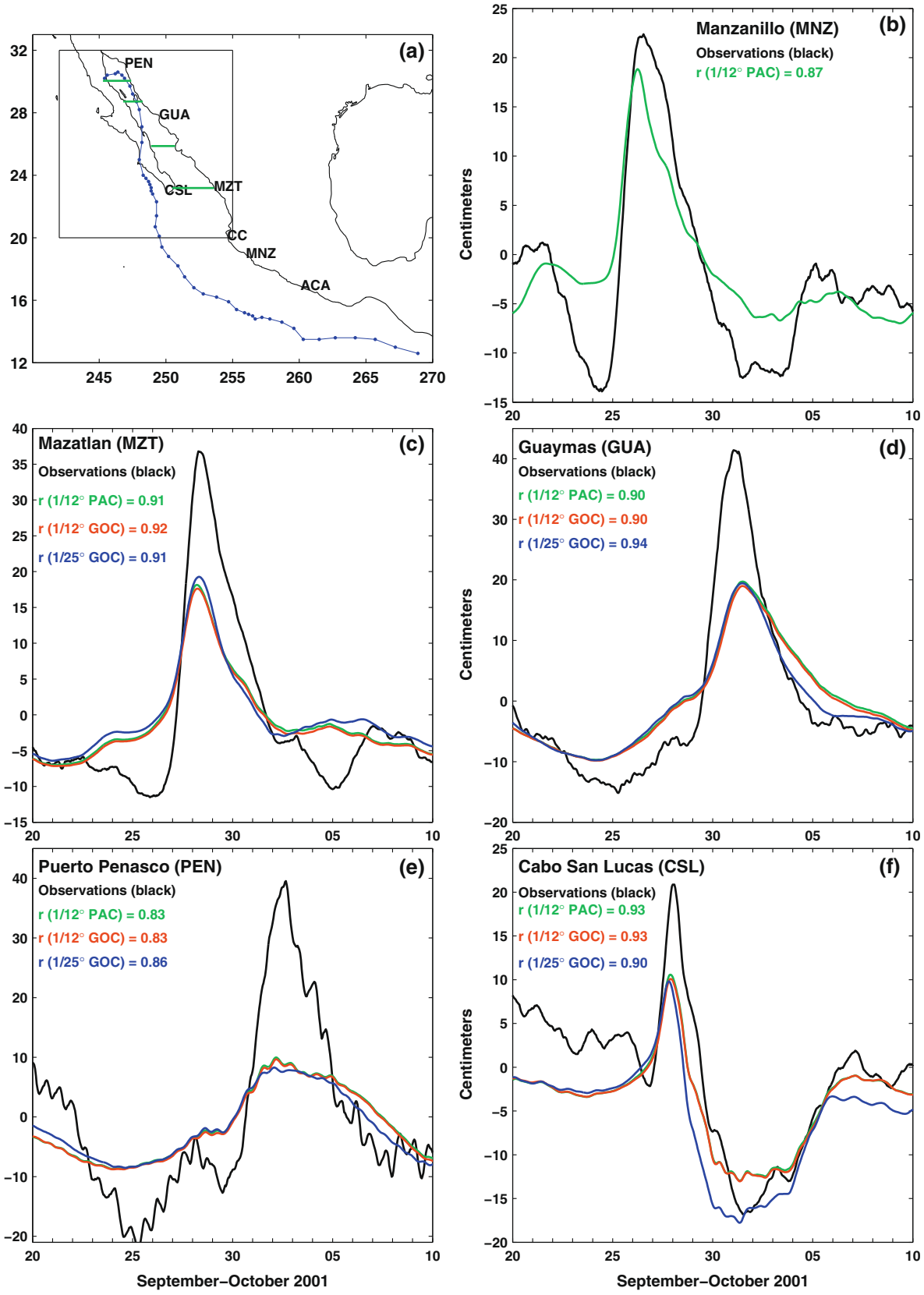

Fig. 1. (a) The path of Hurricane Juliette is represented with the blue line. The locations of Acapulco (ACA), Manzanillo (MNZ), Cabo Corrientes (CC), Mazatlán (MZT), Guaymas (GUA), Puerto Peñasco (PEN), and Cabo San Lucas (CSL) are indicated. The black rectangle indicates a domain of the 1/12° GOC and 1/25° GOC nested HYCOM. The four green west-east lines inside of the GOC indicate the positions of the cross-sections where the transport of Fig. 8 is calculated. Time series of observed (black line) and 1/12° Pacific, 1/12° and 1/25° GOC HYCOM simulated (green, red, and blue lines, respectively) sea level at: (b) Manzanillo, (c) Mazatlán, (d) Guaymas, (e) Puerto Peñasco, and (f) Cabo San Lucas. The observed data have been de-tided, corrected for atmospheric pressure loading effects and a 1-day running mean filter has been applied. The correlation coefficient (r) between the observed and simulated time series is indicated.

exploits the HYCOM to HYCOM nesting capability to simulate the GOC response to Hurricane Juliette.

The upper-ocean (0–100 m) mean circulation at the entrance of the GOC is characterized by eastern boundary poleward currents along the western coast of mainland Mexico and by western boundary equatorward currents along the eastern coast of the Baja California Peninsula (Castro et al., 2000; Zamudio et al., 2008). However, the model results of this study show that: (1) Hurricane Juliette's winds reversed this mean circulation generating strong poleward coastal-attached currents along the eastern coast of the Baja California Peninsula, (2) Juliette's winds induced strong variability in the volume transport at the entrance of the GOC, (3) Juliette's winds forced strong upwelling along the southwestern coast of the GOC, and (4) Juliette's winds generated a CTW, which was measured by several tide gauges along the coast. During its propagation this CTW modulates the evolution of the upwelling forced by Juliette at the entrance of the GOC.

2. Model

HYCOM is the HYbrid vertical Coordinate Ocean Model, which is isopycnal in the open stratified ocean, terrain-following in shallow coastal regions, and *z*-level in mixed layer and unstratified regions. This generalized vertical coordinate approach is dynamic in space and time via the layered continuity equation that allows a smooth dynamical transition between the coordinate types. HYCOM (Bleck, 2002) was developed from the Miami Isopycnic Coordinate Ocean Model (MICOM) using the theoretical foundation for implementing a hybrid coordinate system (Bleck and Benjamin, 1993). Since a single vertical coordinate (depth, density, or terrain-following sigma) cannot by itself be optimal everywhere in the ocean, the hybrid approach is an option that uses the best of the three vertical coordinates depending of the ocean characteristics. HYCOM application to the Pacific and Gulf of California modeling has been discussed by Metzger et al. (2004), Zamudio et al. (2004), López et al. (2005), Cheng et al. (2007), Kelly et al. (2007), Kara et al. (2008), and Zamudio et al. (2008).

The eddy-resolving (1/12° equatorial resolution) Pacific HYCOM domain extends from 20°S to 65.8°N and from 98.9°E to 77.6°W, and both the 1/12° and 1/25° nested GOC HYCOM domains extend from 118°W to 105°W and from 20°N to 32°N. The geographical extension of these two nested GOC models is indicated by a black rectangle in Fig. 1a. Note that the GOC HYCOM domain is larger than the real GOC. These three HYCOM configurations are identically forced with 1° horizontal resolution six-hourly winds and daily averaged heat fluxes from the Fleet Numerical Meteorology and Oceanography Center's Navy Operational Global Atmospheric Prediction System (NOGAPS) (Rosmond et al., 2002), and they include monthly rivers and turbidity forcing (Kara et al., 2005a,b,c). Pacific HYCOM ran for all of 2001 while the nested GOC HYCOM simulations integrate over September and October 2001. In addition, the models include realistic bottom topography and coastline geometry that are based on a modified version of the 1/30° NRL DBDB2 topography (http://www.7320.nrlssc.navy.mil/DBDB2_WWW). The models use the 10 meter isobath as a land-sea boundary, include 20 vertical coordinate layers, allow isopycnals to intersect sloping topography by allowing zero thickness layers, and do not include ocean data assimilation. In addition, the models include five different embedded ocean mixed layer sub-models, which can be used to simulate the variability of the mixed layer. In this particular study, the K-Profile Parameterization mixed layer model of Large et al. (1994) is used.

Initial and lateral boundary conditions for the nested GOC regional models are provided by Pacific HYCOM. The different regional applications and the model-data comparisons included in the works of Prasad and Hogan (2007), Barth et al. (2008a,b,c),

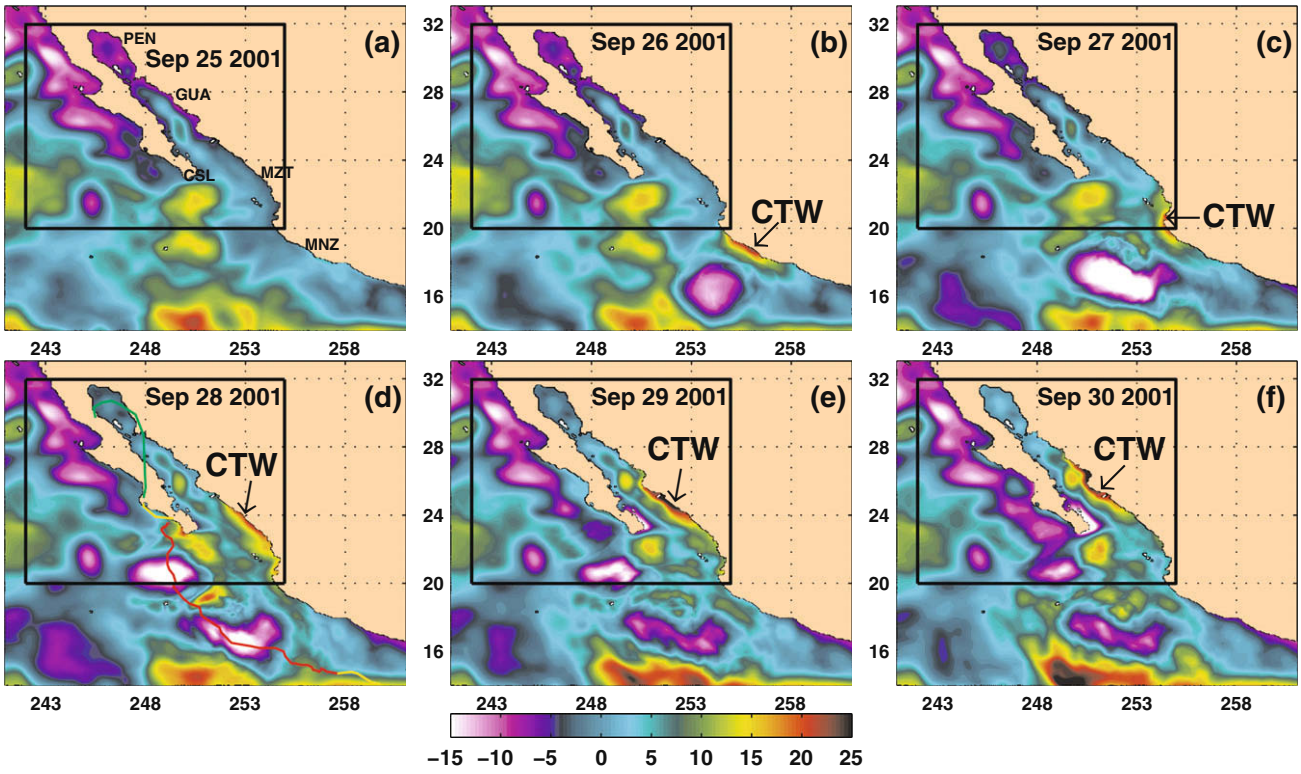

Fig. 2. Sea surface height snapshots (color contours in cm) over a subregion for six different dates in September 2001 as simulated by 1/12° Pacific HYCOM forced by NOGAPS 6 hourly winds and daily averaged thermal forcing. The different positions of the coastally trapped wave (CTW) are indicated. The black rectangle indicates a domain of the 1/12° and 1/25° GOC nested HYCOM.

Zamudio and Hogan (2008), Zamudio et al. (2008), Kourafalou et al. (2009), Halliwell et al. (2009), Gierach et al. (2009), and Han et al. (2009) provide some validation for the use of the HYCOM nesting capability (regional-ROMS or regional-HYCOM inside global or basin scale HYCOM).

3. Results and discussion

This section is divided in two subsections. The first one is devoted to the study of the generation and propagation of the downwelling CTW forced by Juliette along mainland Mexico. Since, this wave plays a key role on the modulation of the coastal upwelling generated by Juliette at the entrance of the GOC, the accuracy in the simulation of this CTW is essential. Thus, a suite of numerical simulations is analyzed. All these simulations are nested inside of Pacific HYCOM and differ in horizontal resolution, extension of the nested domain, and resolution of the wind product used to force the model. The second subsection includes the circulation, volume transport, and coastal upwelling forced by Juliette and the role of the mainland CTW in the evolution of the coastal upwelling.

3.1. The mainland coastally trapped wave

3.1.1. Generation and propagation

Juliette's coastal poleward winds generated a baroclinic CTW between Acapulco and Manzanillo that was clearly measured (maximum amplitude of ~22 cm) by the tide gauge at Manzanillo, and simulated (maximum amplitude of ~19 cm) by Pacific HYCOM (Fig. 1b). Juliette's winds continued forcing the CTW and consequently it propagated poleward as a forced CTW entering the GOC HYCOM domain (represented by a black rectangle in Fig. 1a) through the southern open boundary on September 26 (Fig. 2). In addition, the wave increased its maximum amplitude to ~40 cm (measured) and ~20 cm (simulated) in the tide gauge measurements at Mazatlán, Guaymas, and Puerto Peñasco (Fig. 1c–e). This error of 50% in the simulated amplitude of the CTW is reduced in the results presented in Section 3.1.4. The alongshore and cross-shore scales of the CTW simulated by Pacific HYCOM were ~580 km and ~64 km, respectively (Fig. 2). The wave phase speed was ~2.7 m/s and it generated near-shore, near-surface currents >1 m/s, and subsurface currents >0.50 m/s. Furthermore, Hurricane Juliette generated a second CTW along the southern tip of the west coast of the Baja California Peninsula (BCP) that is clearly recognized in the tide gauge observations at Cabo San Lucas (maximum amplitude of ~21 cm), and the model simulations (maximum amplitude of ~10 cm) (Figs. 1f and 2d). After its generation, this second CTW propagated northward and was rapidly weakened (Fig. 2d–f) by Juliette's upwelling favorable winds. Consequently, only remnants of this CTW exit the GOC model domain through the northern boundary of the West Coast of the BCP. Thus, this second CTW is not well suited for studying its effects inside of the GOC. In fact, this wave never enters the GOC. But, the first CTW generated by Hurricane Juliette (as well as the hurricane itself) originated outside of the black nested domain of Fig. 1a and both entered into the nested GOC domain as well-defined signals through the southern boundary (Fig. 2).

Note that the phase of the first and the second CTWs is well simulated (correlation coefficients >0.90 for Mazatlán, Guaymas, and Cabo San Lucas, and >0.83 for Puerto Peñasco) by the three different model simulations of Fig. 1. Nevertheless, those simulations underestimate the amplitude of the two waves. Why is the amplitude of the two waves underestimated by Pacific and GOC HYCOM? The regional GOC HYCOM is nested inside of Pacific HYCOM and an intrinsic problem of the nested approach is that some level of error is always introduced across the open boundaries used to transmit the oceanic signals from the larger domain to the nested domain. Then, the underestimation of the amplitude of the two waves could be due to the nested boundaries, and/or the 1° resolution of the atmospheric forcing, which is not fine enough to simulate the small wind scales generate by Hurricane Juliette. Model results, which validate the nesting approach and the use higher resolution winds to force the regional ocean models are presented and discussed in the next three subsections.

3.1.2. Validation of the nesting approach

If the existence of high-resolution regional ocean models (nested inside of lower-resolution models) is in part due to the ability of these models to simulate short time and space scale processes at relatively low computational cost, then what is the value of the 1/12° GOC simulation nested inside of the 1/12° Pacific

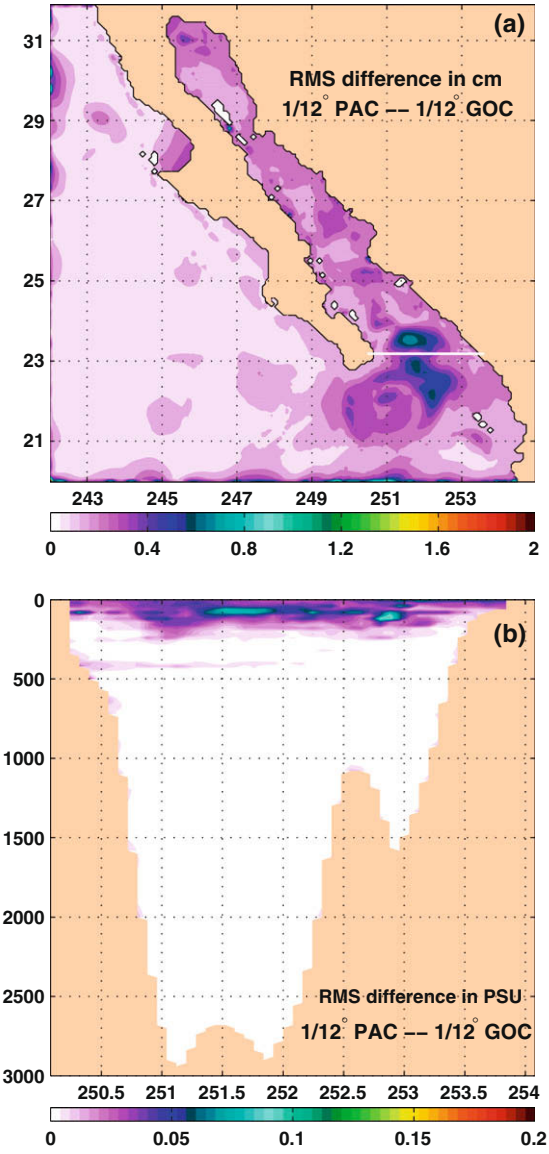

Fig. 3. (a) Sea surface height root mean square (RMS) difference (color contours in cm) between 1/12° Pacific HYCOM and 1/12° nested GOC HYCOM over the GOC domain. (b) Salinity RMS difference (color contours in PSU) between 1/12° Pacific HYCOM and 1/12° nested GOC HYCOM over a cross-section along the white west-east line at the entrance of the GOC, which is indicated in panel (a). Both panels cover the period September and October 2001.

simulation? In the case of the 1/12° experiments (green and red time series in Fig. 1b–f) the nested GOC and the Pacific configurations have the same horizontal and vertical resolution (1/12°, and 20 layers, respectively). Thus, considering that the GOC and the Pacific models have identical forcing, any difference between the simulations is due to the nested boundaries. Also, at 1/12° resolution the results of the GOC configuration can be compared and validated (one to one) with the results of the Pacific configuration. Here, we use a root mean square (RMS $= \sqrt{\frac{\sum_{i=1}^{n}(PAC_i - GOC_i)^2}{n-1}}$), where PAC and GOC are the results from the Pacific and Gulf of California simulations, respectively, n is number of data points, and i is time (space) if producing a map (time series) as a measure of error. It will be used to find the boundary condition parameters that produce the smallest RMS and most accurately preserve the CTW as it propagates through the nested GOC boundaries.

Two examples of the RMS difference obtained are shown in Fig. 3. That includes the SSH RMS difference between the 1/12° nested GOC model and the 1/12° Pacific model over the GOC domain for September and October 2001 (Fig. 3a). The basin-wide RMS difference is <1 cm and this is small compared to the actual SSH range (−15 to 40 cm) and with the CTW amplitude >35 cm (Figs. 1 and 2). In addition, we calculate the salinity RMS difference between the 1/12° nested GOC model and the 1/12° Pacific model over a cross-section along a west-east line at 23.2°N (close to the entrance of the GOC) for September and October 2001 (Fig. 3b). That shows a maximum RMS error (<.1 PSU) close to the sea surface, but the RMS error in most of the cross-section is ∼0, which means that for most of the water column, the 1/12° nested GOC model reproduces the salinity field simulated by the 1/12° Pacific model during September and October 2001. Later, the boundary condition parameters (which produce the smallest RMS difference) were used in 1/25° GOC nesting experiments.

3.1.3. The 1/25° nested GOC

Since our interest in nested high-resolution regional models is based on their ability to simulate short-scale processes at low computational cost, then a 1/25° nested GOC model was configured for the domain indicated by the black rectangle in Fig. 1a. Thus, the only difference between the red (1/12°) and blue (1/25°) time series in Fig. 1c–f is the horizontal grid resolution. The time series and correlation coefficients of Fig. 1c–f show, in essence, the same degree of accuracy for the propagation of the wave into both the 1/12° and 1/25° nested models. That is supported by the SSH snapshots on September 29, 2001, which show similar horizontal and vertical features and basically the same geographical location for the CTW simulated by 1/12° Pacific, 1/12° GOC, and 1/25° GOC (Fig. 4). In addition, note the lack of significant differences between the amplitude of the CTW simulated with the 1/12° and 1/25° GOC models, which indicates that the 1/12° resolution is fine enough to resolve this wave and to resolve the Rossby radius of deformation of ∼30 km of the GOC region. However, it is important to keep in mind the intrinsic limitations of the simulations. In order to simulate the evolution of CTWs it is necessary to incorporate the shelf's topography and coastline's variations as accurately as possible, and clearly the 1/12° or even the 1/25° resolution can not incorporate the small features of the capes around which the CTW propagates.

3.1.4. 1° NOGAPS versus 27 km COAMPS forcing

The results and discussion included in Sections 3.1.2 and 3.1.3 suggest that the underestimation of the amplitude of the mainland CTW is due to the 1° resolution of the atmospheric forcing and not the 1/12° resolution of the ocean model. We develop two new experiments to provide some insight on the effects of the atmospheric forcing resolution on the amplitude of that CTW. In these experiments we use two different resolutions for the atmospheric forcing: 1° NOGAPS (which is the forcing used in the three simulations of Figs. 1–4) and 27 km Central America Coupled Ocean Atmosphere Prediction System (COAMPS). The horizontal resolution is 1/25° and in these two experiments the GOC HYCOM domain extends from 118°W to 105° W and from 14°N to 32°N (the geographical extension of these nested GOC models is indicated by the red rectangle in Fig. 5a). Hence, Hurricane Juliette's CTW forms within the new GOC domain and does not have to be passed across any nested boundary and consequently no error can be attributed to the presence of nested boundaries.

Fig. 5 includes observed and simulated SSH at four different locations along the West Coast of mainland Mexico and at one location on the tip of the BCP. In general, there is fair qualitative and quantitative (correlation coefficients ranging from 0.83 to 0.97) agreement between the observed and simulated phase (within all the experiments) of the CTW. But is there any progress in the simulation of the amplitude of the CTW? The three experiments of Fig. 1 clearly underestimate the amplitude of the wave. Increasing the resolution of the wind forcing (from 1° NOGAPS (blue time series in Fig. 5b–f) to 27 km COAMPS (red time series)) led to a large improvement in the simulated SSH along the Mexican west coast stations (from Manzanillo to Puerto Peñasco), with the station at Guaymas (Fig. 5d) showing the largest improvement in the amplitude of the CTW. It is important to note that the improvement in the simulation of SSH is not due to the difference in the domain extent (compare Fig. 1a versus Fig. 5a), since the SSH response is

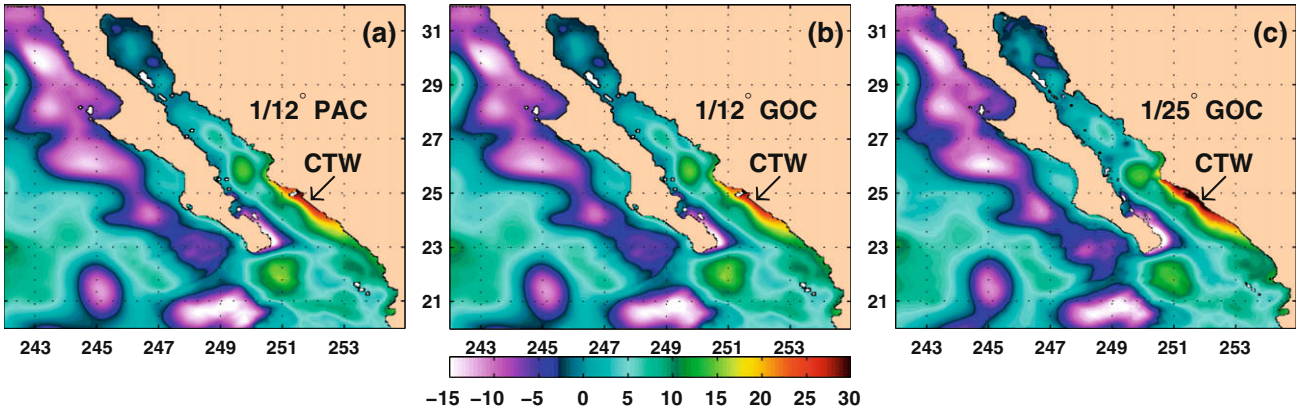

Fig. 4. Sea surface height snapshots (color contours in cm) for September 29, 2001 simulated with: (a) 1/12° Pacific HYCOM, (b) 1/12° GOC HYCOM, and (c) 1/25° GOC HYCOM. The coastally trapped wave (CTW) was generated by Hurricane Juliette outside of the nested region and entered into the nested GOC models through the southern boundary.

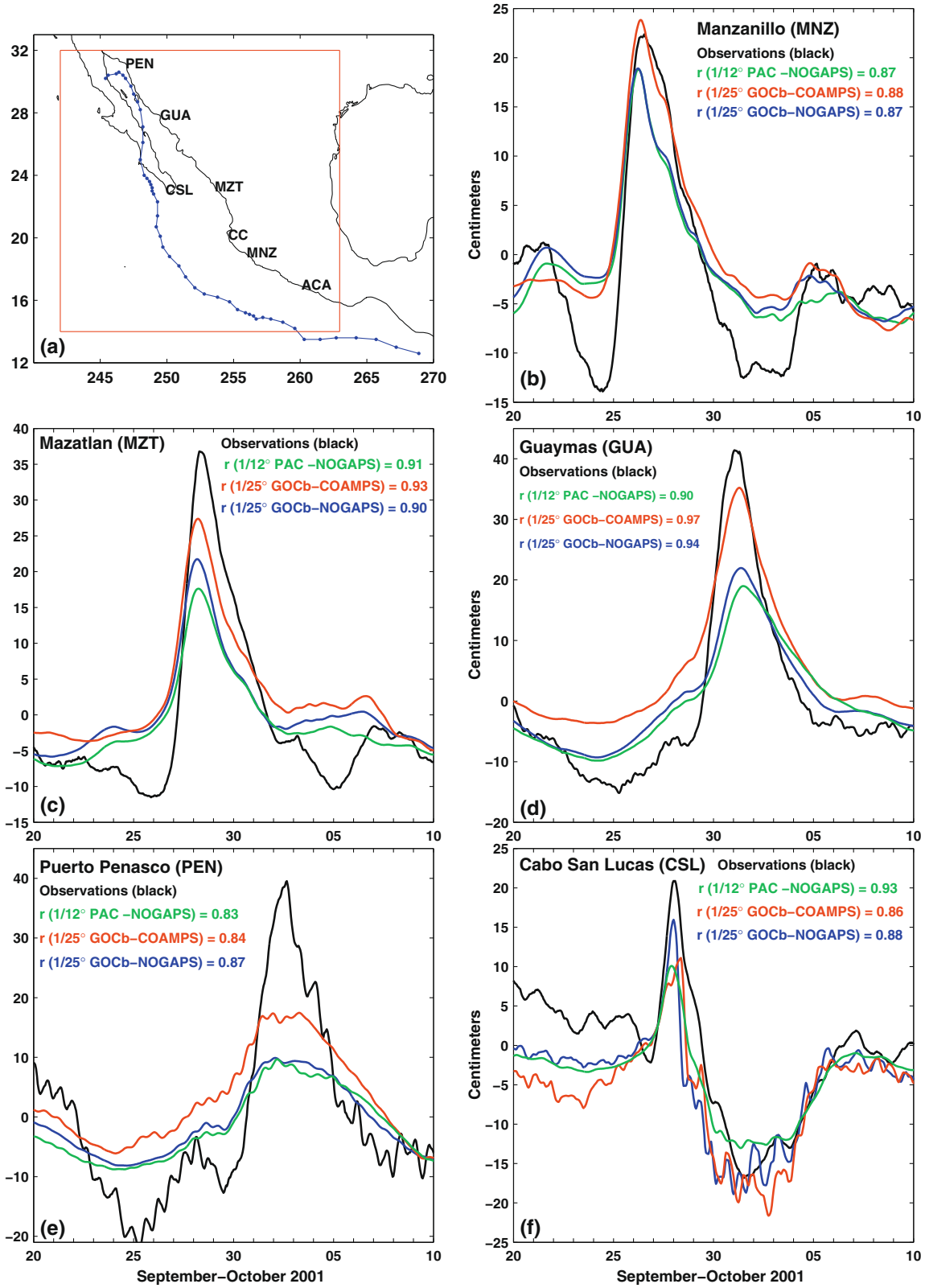

Fig. 5. (a) The path of Juliette is represented with the blue line. The locations of Acapulco (ACA), Manzanillo (MNZ), Cabo Corrientes (CC), Mazatlán (MZT), Guaymas (GUA), Puerto Peñasco (PEN), and Cabo San Lucas (CSL) are indicated. The red rectangle indicates a domain of the 1/25° GOC nested HYCOM. Time series of observed (black line) and 1/12° Pacific HYCOM (green line forced by 1° NOGAPS), 1/25° GOC HYCOM (red line forced by 27 km COAMPS), and 1/25° GOC HYCOM (blue line forced by 1° NOGAPS) simulated sea level at: (b) Manzanillo, (c) Mazatlán, (d) Guaymas, (e) Puerto Peñasco, and (f) Cabo San Lucas. The observed data have been de-tided, corrected for atmospheric pressure loading effects and a 1-day running mean filter has been applied. The correlation coefficient (r) between the observed and simulated time series is indicated.

similar in the two domains when using NOGAPS forcing as shown by the blue time series of Figs. 1c–e and 5c–e. Over all, the improvement in the amplitude of the CTW is due to the increase in the resolution of the atmospheric forcing, which on 27 km grid COAMPS is better able to simulate the small wind scales generated by Hurricane Juliette than can 1° resolution NOGAPS (not shown).

3.2. Upper-ocean currents, transport, and upwellings generated by Juliette

3.2.1. Upper-ocean currents and transport

The upper-ocean mean currents at the entrance of the GOC are characterized by broad and weak poleward eastern boundary currents along mainland Mexico that are compensated by narrow and strong equatorward western boundary currents along the eastern coast of the BCP (Fig. 6a). Although these mean currents have a strong seasonal fluctuation, the equatorward currents attached to the eastern coast of the BCP prevail throughout the year as displayed in the monthly means of Fig. 4 in Zamudio et al. (2008). However, this upper-ocean circulation was strongly altered by Hurricane Juliette. During the four days of its passage, Juliette's winds blew poleward along the entrance of the GOC (Fig. 7). Those winds reversed the direction of the western boundary currents along the eastern coast of the BCP (from equatorward to poleward) as evidenced by the instantaneous upper-ocean currents on September 28, 2001, which are mostly strongly poleward (Fig. 6b). Since, these poleward flows were maintained for several days, they generated a strong coastal baroclinic jet along the eastern coast of the BCP (Fig. 6c). Note the reversal feature between the long-term and nine-day upper-ocean mean currents of Fig. 6a and c (respectively) and how the currents along the eastern coast of the BCP are basically mirror images with opposite signs.

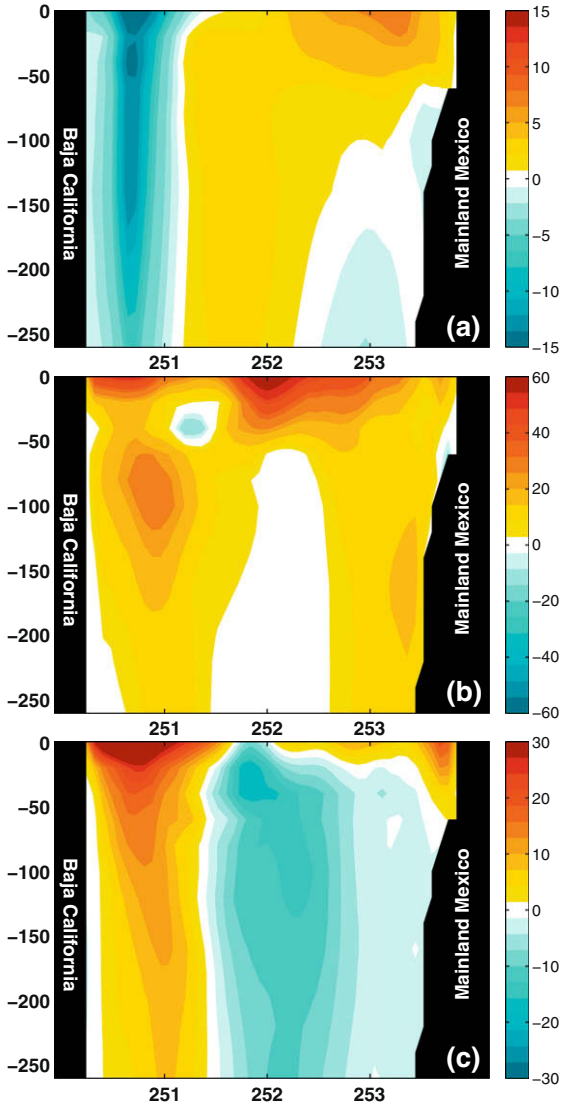

Fig. 6. Meridional currents (color contours in cm/s) simulated with HYCOM over the cross-section indicated in Fig. 3: (a) 7-year mean (adapted from Zamudio et al. (2008)), (b) instantaneous currents on September 28, 2001, and (c) 9-day mean for the period September 25 to October 3, 2001. Positive currents indicate northward flow.

Juliette's poleward winds not only reversed the upper-ocean currents, they also generated a strong northward transport at the entrance of the GOC (Fig. 8). This transport decreases northward, but it is simulated as far north as 30°N. Since the GOC is a semi-enclosed sea, then over time scales of days the imbalance in volume storage in the GOC is close to zero. Nevertheless, Juliette's winds forced at the entrance of the GOC a northward transport of more than 0.2 Sv on September 28, 2001. After the northward transport ceased an equally intense southward transport was produced to balance the excess of water introduced by the northward transport (Fig. 8). Strub and James (2002) and López et al. (2005) reported fluctuations in the transport along the complete entrance of the GOC due to the 1997 El Niño event and the passage of equatorially generated intraseasonal CTWs. That means those transport variations were indirectly induced by remote equatorial winds. Now, Fig. 8 shows model evidences of the direct effect of the wind on the transport at the entrance of the GOC.

3.2.2. Coastal upwellings

When Hurricane Juliette was approaching the GOC, the winds along the southeastern coast of the BCP changed from basically no wind on September 25–26, to augmented upwelling favorable winds on September 27, to strong upwelling favorable winds on September 28–30 (Fig. 7). A snapshot sequence of temperature cross-section along a west-east line at 23.2°N (close to the entrance of the GOC) illustrates the upwelling event (Fig. 9). On September 25 and 26 the temperature field is characterized by a strong horizontal stratification and a shallow mixed layer along the complete cross-section (Fig. 9a and b). In particular, close to the BCP coast the thermocline (based on the observations of Castro et al. (2000, 2006) the depth of the 20 °C isotherm is used as an indicator of the depth of the thermocline in the present study) and the base of the mixed layer were located at ~60 m and ~5 m depth, respectively. In contrast, close to the coast of mainland Mexico the thermocline and the base of the mixed layer were located deeper at ~90 m and ~20 m, respectively. Those are signatures of the coastal-attached poleward Mexican Coastal Current (Zamudio et al., 2007, 2008; Godínez et al., in press). Next, on September 27 Juliette neared the BCP (Fig. 7) generating a weak cooling in the upper ~20 m of the water column and a deepening of ~10 m in the mixed layer. Those effects are more evident close to the BCP coast (Fig. 9c). A day latter, Juliette get closer to the BCP (Fig. 7) and forced a transient downwelling close to the BCP coast that moved the thermocline and the base of the mixed layer to ~80 m and ~30 m depth, respectively (Fig. 9d). However, close to the coast of mainland Mexico a downward movement of the thermocline was occurring at this time as shown by the deeper thermocline in Fig. 9d than in Fig. 9a–c. This downwelling effect is expected, because of the onshore Ekman transport induced by the wind along this coast and because the mainland downwelling CTW (which is characterized by the downward movement of the thermocline during its propagation) is propagating along the southeastern coast of the GOC during September 28 (Fig. 10).

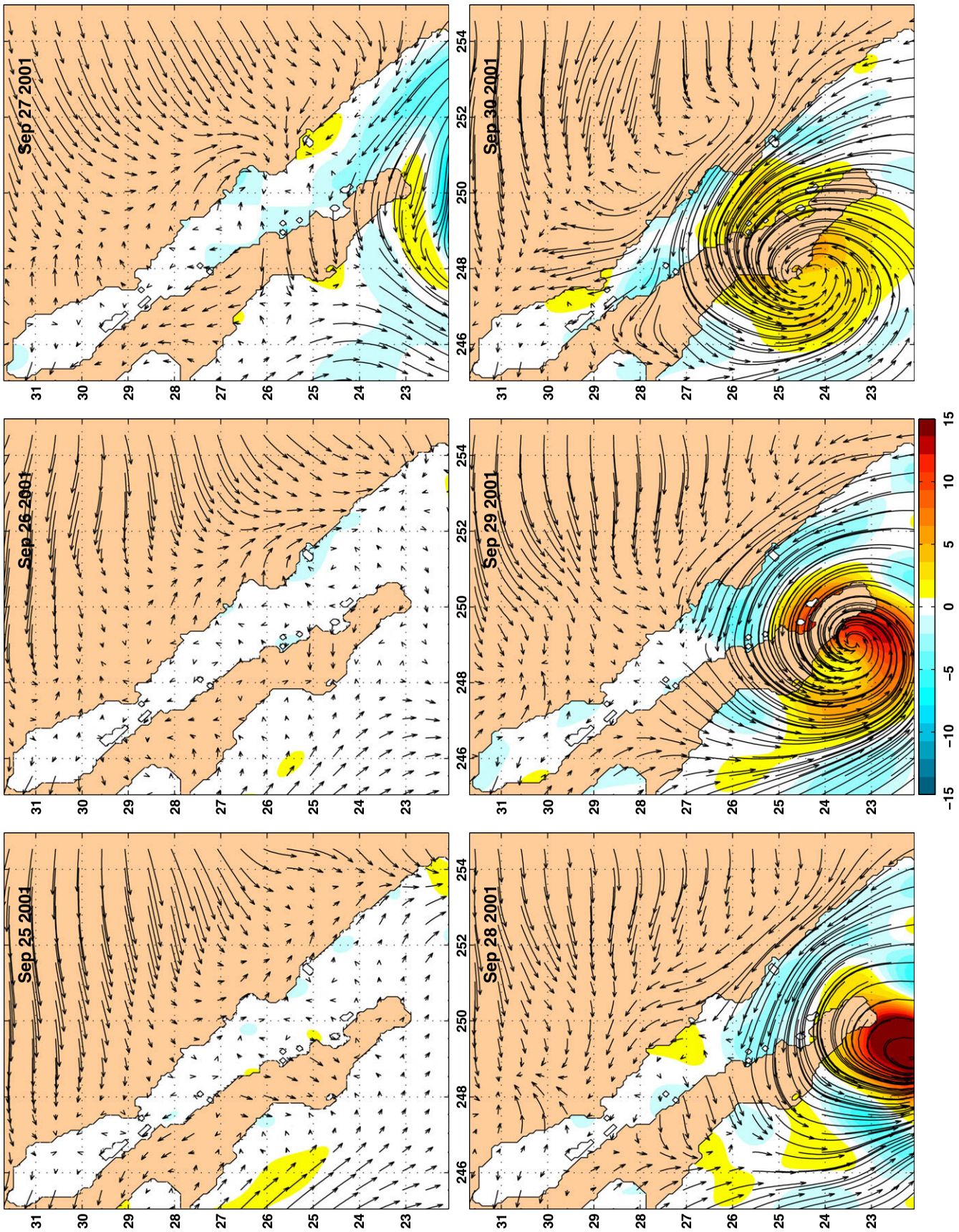

Fig. 7. Wind stress curl (color contours in 1×10^{-6} Pa/m) and wind stress (vectors) for six different dates in September 2001 as determined by 1° NOGAPS.

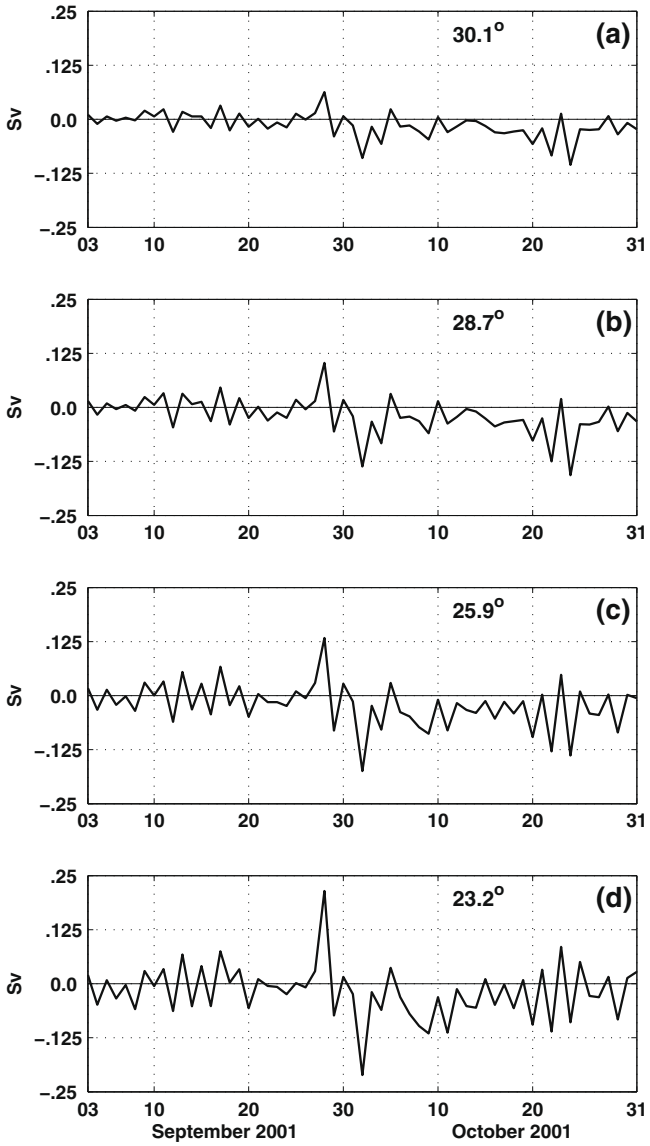

Fig. 8. Time series of transport (in Sv) over cross-sections along the four different west-east lines of Fig. 1. Positive transport indicates northward flow. The latitude of the cross-sections is indicated.

From September 29 to October 3 Juliette's winds generated a strong offshore Ekman transport along the southeastern coast of the BCP, deepened the mixed layer to ~40 m depth in some regions along the cross-section, and forced a strong upwelling event that generated a vertical velocity > 30 m/day while raising the thermocline to ~20 m depth in 2 days (Fig. 9d–f). It also created and maintained a strong upwelling front for several days as evidenced by the upward slope of the isotherms towards the BCP coast from September 29 to October 3 (Fig. 9f–i). In addition, note the distribution of the thermocline at ~252° on October 3 (Fig. 9i). That could be indicative of Juliette generated internal waves as disscused by Gill (1984) for internal waves induced by any moving storm and by Keen and Allen (2000) and Jaimes and Shay (in press) for internal waves forced by Hurricanes Andrew, Katrina, and Rita, respectively.

It is interesting to note that even though Juliette's winds forced a strong upwelling, they did not ventilate the thermocline and generate "Full Upwelling" as defined by Csanady (1977). Why did Juliette not generate a "Full Upwelling" along the eastern coast of the BCP? A plausible answer to this question is as follows. Fig. 10 includes a snapshot sequence of subsurface (150 m depth) currents showing the currents forced by Juliette and the currents associated with the evolution of the mainland CTW inside of the GOC. Those two features are indicated by the yellow sign "JC" and the white sign "CTW", respectively. The subsurface currents on September 27 neither include evidence of the presence of the CTW nor of Juliettes's currents (Fig. 10a). The CTW arrives to the GOC on September 28 and it is characterized by subsurface alongshore currents with maximum speeds of ~50 cm/s. During this day Juliette's subsurface currents are not evident yet (Fig. 10b). Next, from September 29 to October 1, the CTW continues its northward propagation interacting with the capes and ridges along the eastern coast of the GOC. At the same time, Juliette forced strong poleward subsurface currents along the southwestern coast of the GOC (Fig. 10c–e). By October 2 the CTW reaches the shelf break between 28°N and 29°N when a significant part of the CTW reversed the direction and propagated equatorward along the western coast of the GOC. The region of this reversal is indicated by the yellow sign "CTW" in Fig. 10f. The reversal of a CTW propagating along the coast of the GOC was previously modeled by Martínez and Allen (2004). Furthermore, the Juliette induced poleward subsurface currents along the southwestern coast of the GOC prevail as well-defined signal at this time (Fig. 10f–g). However, on October 3 the CTW reaches the southwestern coast of the GOC and starts to interact with the Juliette's poleward currents. Finally, from October 4 to October 5 the CTW propagates around the southern tip of the Baja California Peninsula opposing and partially weakening the Juliette induced poleward subsurface currents and the development of the "Full Upwelling".

The inclusion of the mixed layer depth in the temperature cross-sections of Fig. 9 facilitates the visualization/separation of the temperature fluctuations due to mixing and/or upwellings. That is not a trivial separation when both mixing and upwelling are induced by the same hurricane in the same region (Babin et al. 2004). Thus, the Juliette induced-upwelling injected cold nutrient-rich subsurface water into the euphotic zone. Next, the sunlight stimulated phytoplankton growth producing a phytoplankton-bloom and this bloom was measured by the SeaWIFS satellite as elevated concentrations of chlorophyll-a along the southeastern coast of the BCP (Fig. 11). Note the low concentration of chlorophyll-a during the period September 25–28, along the southeastern coast of the BCP, and how this chlorophyll-a concentration increases dramatically under the influence of the Hurricane Juliette (September 29 and 30). After the passage of the hurricane the chlorophyll-a concentration decreases slowly returning to a level closest to a pre-Juliette level in ~3 weeks (not shown). To the best of our knowledge, Figs. 9 and 11 represent the first modeling and observational evidence for the existence of hurricane-induced upwelling along the east coast of the BCP. However, they are not rare occurrences since this Juliette-induced upwelling and the associated phytoplankton-bloom are similar to the satellite observations reported by Babin et al. (2004) of hurricane-induced phytoplankton blooms in the oceanic desert of the Sargasso Sea region of the North Atlantic. The upper-ocean biophysical response of the Gulf of Mexico to the major hurricanes of 2005 was also reported by Gierach and Subrahmanyam (2008).

4. Summary and concluding remarks

The upper-ocean response of the Gulf of California (GOC) to Hurricane Juliette is studied using two different horizontal grid resolutions (1/12° and 1/25°) of the HYbrid Coordinated Ocean Model (HYCOM). These GOC models are nested inside of the eddy-resolving (1/12° equatorial resolution) Pacific HYCOM, which extends from 20°S to 65.8°N. The latitudinal extent of

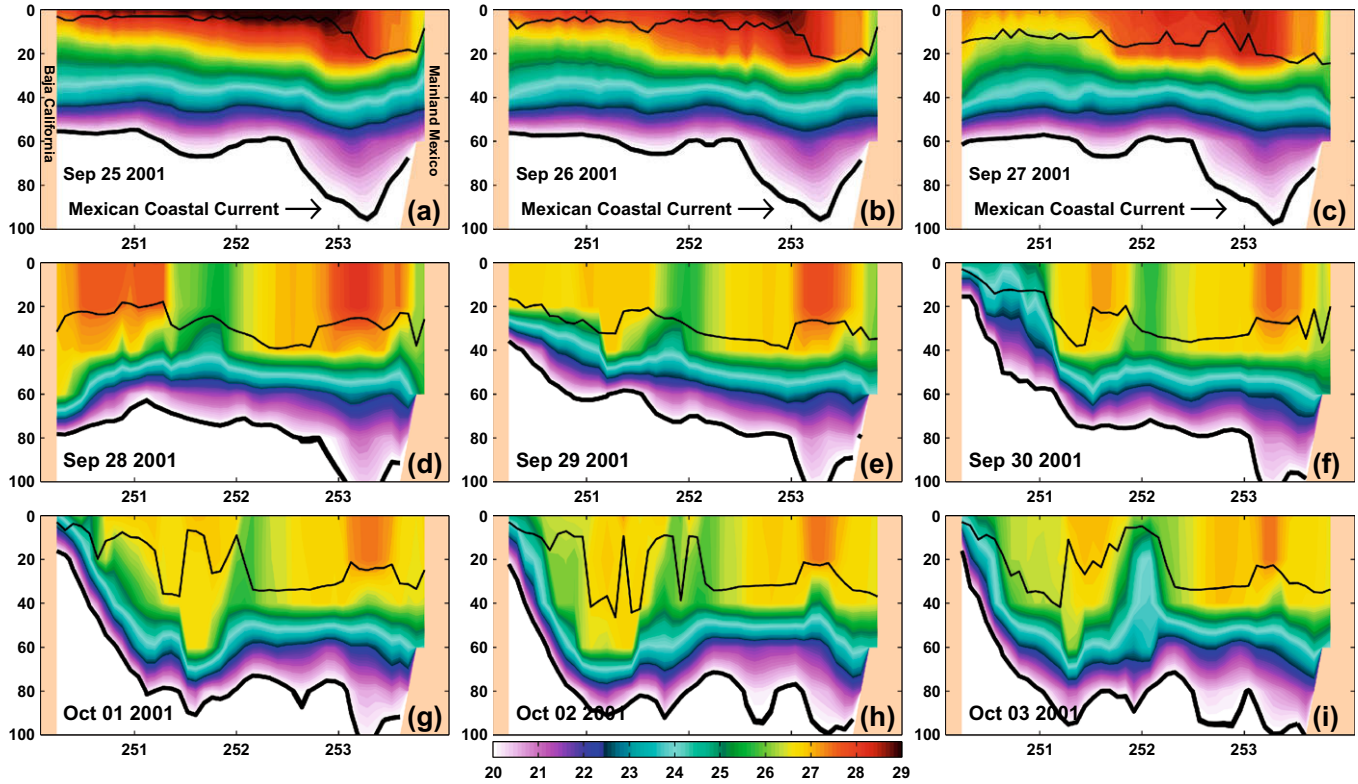

Fig. 9. Temperature (color contours in °C) snapshots for nine different dates in September–October 2001 as simulated with GOC-HYCOM over a cross-section along a west-east line at ~23.2°N (close to the entrance of the GOC), which has the coast of the Baja California Peninsula on the west and the coast of mainland Mexico on the east. To help with the visualization of the Juliette-generated upwelling the 20 °C isotherm (thick black line) is added. The simulated diagnostic mixed layer depth is represented by the thin black line. The signature of the Mexican Coastal Current on the temperature field is indicated in panels (a)–(c).

the Pacific model and the nested GOC approach allow direct examination of the connectivity of the GOC with the Pacific Ocean at high resolution and relatively low computational cost and the free propagation of signals like coastally trapped waves from the Pacific Ocean to the GOC. Thus, the propagation of a Juliette-generated coastally trapped wave (CTW) along the GOC has been studied using two configurations of GOC HYCOM, which are forced with realistic high-frequency winds, heat fluxes, rivers, and turbidity.

To ensure the proper connectivity between the Pacific and the GOC nested models, the sensitivity of the nested boundary condition parameters was examined using a suite of experiments that use the 1/12° nested GOC model for the particular case of the CTW generated by Hurricane Juliette, outside of the GOC domain, and which propagated through the GOC boundaries. Since the nested GOC and the Pacific configurations have the same horizontal resolution (1/12°) and both used the same atmospheric forcing, any difference between the results of the GOC and the Pacific simulations is attributed to the nested boundaries. An advantage of studying the sensitivity of the boundary conditions parameters from the 1/12° GOC model (instead of the 1/25° GOC model) nested inside the 1/12° Pacific model is that the results from the 1/12° GOC configuration can be directly validated (one to one) with the results from the 1/12° Pacific configuration. The results of those simulations were compared and validated (via root mean square difference) with the 1/12° Pacific model, which is the provider of the nested boundary conditions (Fig. 3). Secondly, the sensitivity of the amplitude and phase of the CTW to the atmospheric forcing resolution was investigated using two different wind products (1° resolution NOGAPS and 27 km resolution COAMPS) which was tested in the 1/25° GOC models. The results were compared with sea surface height measured by coastal tide gauges along the west coast of Mexico and they show some improvement in the simulation of the amplitude of the CTW when the COAMPS wind forcing is used. That is an expected result, since the 27 km of resolution is able to better simulate the small wind scales generated by Hurricane Juliette than the 1° resolution NOGAPS.

Model results simulate the well observed (e.g. Castro et al. (2000)) upper-ocean mean circulation at the entrance of the GOC. That is characterized by eastern (western) boundary poleward (equatorward) currents along the southeastern (southwestern) coast of the GOC. However, the direct effect of Juliette's winds reversed this mean circulation and forced a strong poleward coastal baroclinic jet along the southeastern coast of the BCP (Fig. 6). The direct effect of Juliette's winds is also reflected on the northward transport's increment of >0.2 Sv at the entrance of the GOC. Since the GOC is a semi-enclosed sea, after the northward transport ceased an equally intense southward transport was produced to balance the excess of water introduced by the northward transport (Fig. 8). Additionally, Juliette's winds increased the mixed layer depth from ~5 m to ~40 m in some regions along the entrance of the GOC. Moreover, Juliette's winds forced coastal upwellings, which raised the thermocline at the speed of ~30 m/day and generated a upwelling front that lasted several days and was clearly captured by the SeaWIFS chlorophyll-a satellite measurements (Figs. 9 and 11). This Juliette-generated upwelling was partially weakened by the CTW, when it propagated along the southwestern coast of the GOC and interacted with the Juliette's poleward currents (Fig. 10).

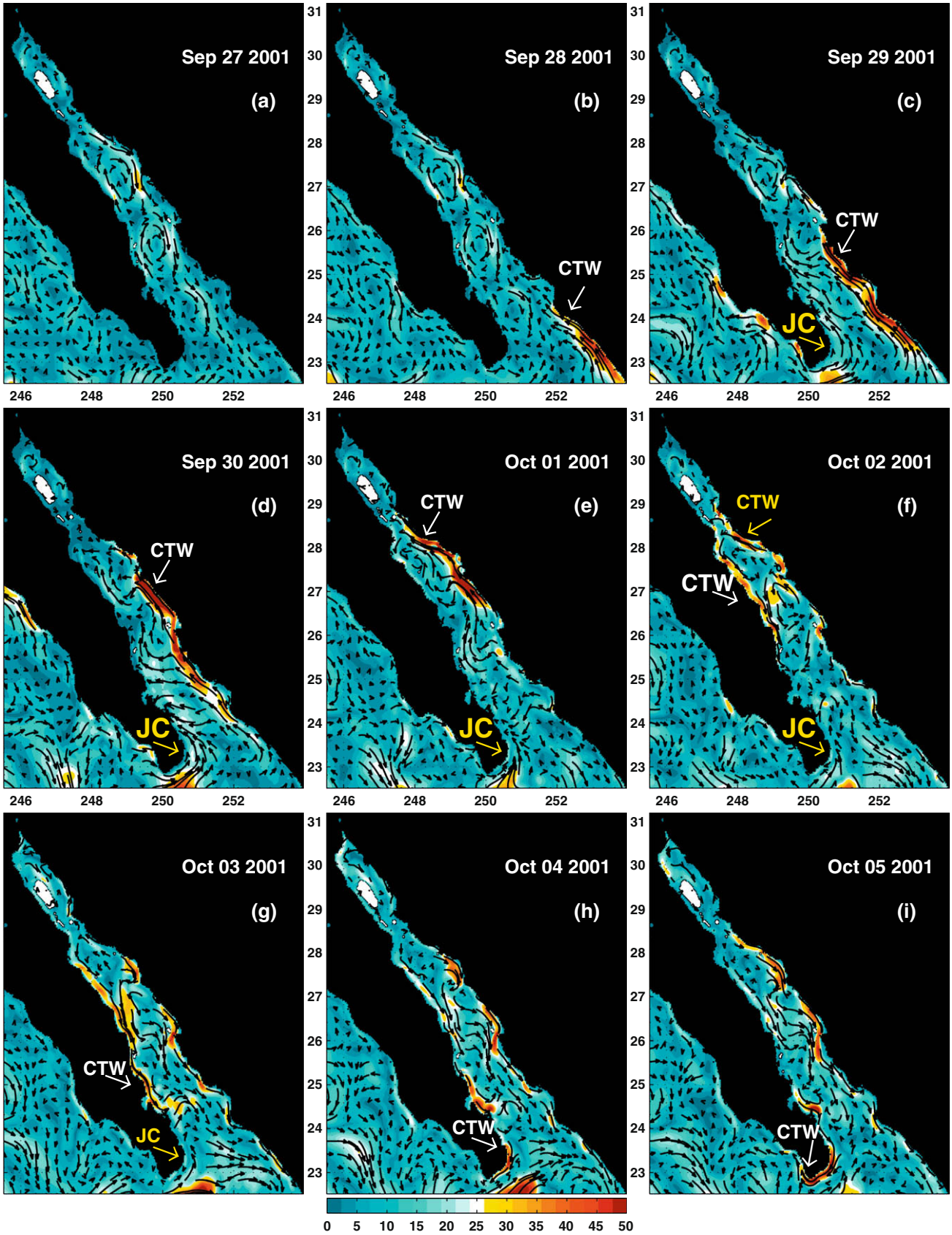

Fig. 10. Subsurface (150 m depth) currents simulated with 1/25° GOC-HYCOM. The color contours (in cm/s) represent the magnitude of the currents and the arrow vectors the direction. The position of the mainland coastally trapped wave is indicated with "CTW" in white letters and the subsurface currents forced by Juliette are indicated with "JC" in yellow letters. The region of the reverse of direction of the coastally trapped wave is indicated with "CTW" in yellow letters. White polygons are model land.

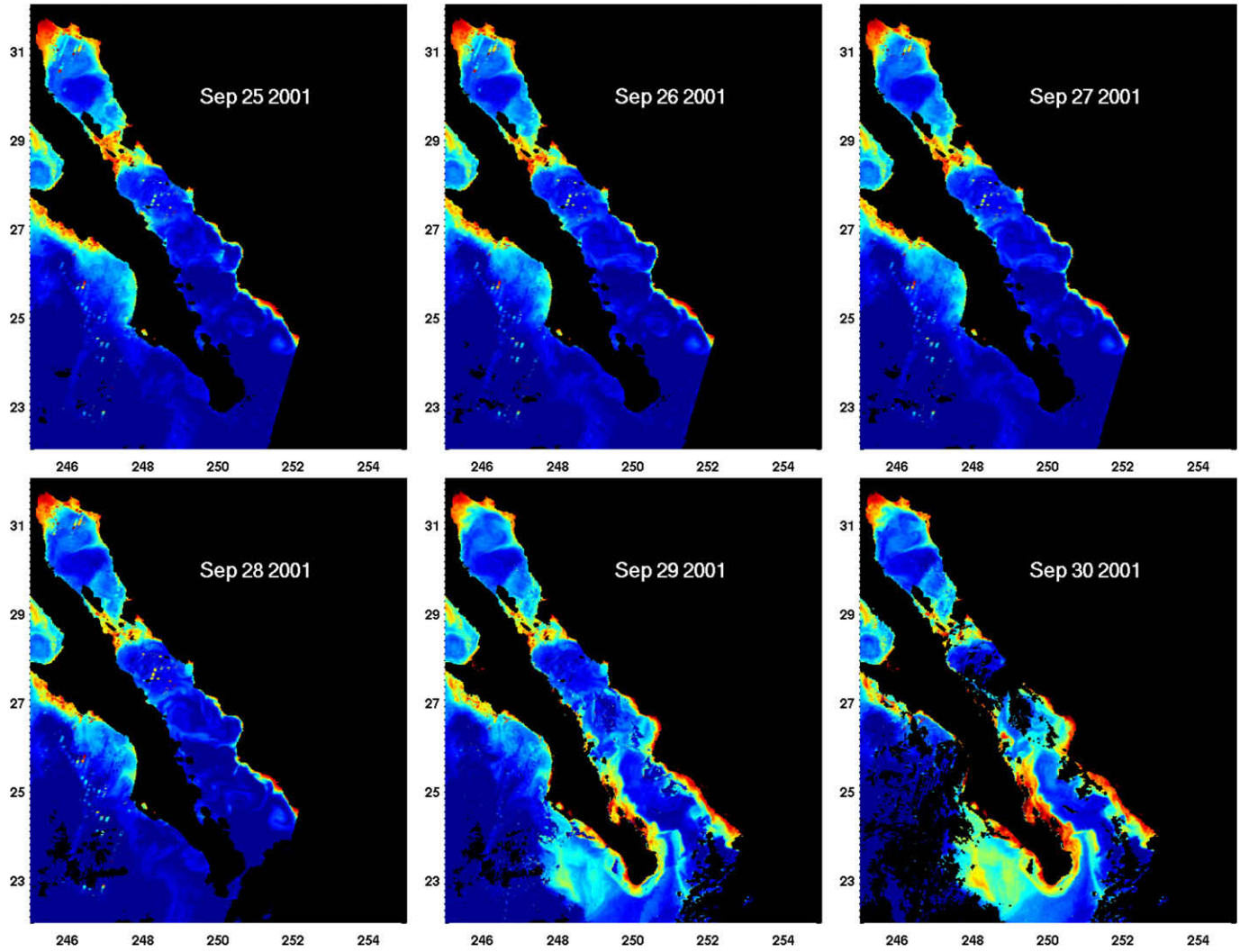

Fig. 11. SeaWiFS chlorophyll-a images for six different dates in September 2001. Blue and green (yellow and red) colors represent low (high) chlorophyll-a concentration. Clouds and land are black. This data was obtained from the NOAA CoastWatch Program (NASA's Goddard Space Flight Center – GeoEye) publicly accessible web site (http://coastwatch.pfel.noaa.gov/infog/SH_chla_las.html).

Acknowledgments

This is a contribution to the projects Coastal Ocean Nesting Studies, Global Remote Litoral Forcing via Deep Water Pathways, Eddy Resolving Global Ocean Prediction including Tides, and Full Column Mixing for Numerical Ocean Models funded by the Office of Naval Research (ONR). The numerical simulations were performed under the Department of Defense High Performance Computing Modernization Program on IBM P4+ computer at the Naval Oceanographic Office, Stennis Space Center. Insightful conversations with Harley Hurlburt and Alan Wallcraft (NRL) help to configure the models and nesting experiments. Jay F. Shriver (NRL) kindly provided the data for the atmospheric pressure load effect used to correct the sea level time series. Thanks are extended to Manuel López, Fernando Miranda, Ignacio González (CICESE), and Jorge Zavala (UNAM) who kindly provided bottom topography data from the northern Gulf of California and the computer codes used to calculate tides, and to plot curly vectors. The sea level data for Manzanillo and Cabo San Lucas was obtained from the publicly accessible web site (http://uhslc.soest.hawaii.edu) of the University of Hawaii Sea Level Center, and the sea level data for Mazatlán, Guaymas, and Puerto Peñasco was kindly provided by the Mexican Navy. Thanks are extended to two anonymous reviewers, the Ocean Modelling editors Will Perrie and Stephen Griffies, and Benjamin Jaimes (RSMAS) for their constructive comments, suggestions, and corrections, which greatly improved the manuscript. This paper is NRL Contribution No. NRL/JA/7320/09/0107.

References

Amador, J.A., Alfaro, E.J., Lizano, O.G., Magaña, V.O., 2006. Atmospheric forcing of the eastern tropical Pacific: a review. Progress in Oceanography 69, 101–142.

Babin, S.M., Carton, J.A., Dickey, T.D., Wiggert, J.D., 2004. Satellite evidence of hurricane-induced phytoplankton blooms in an oceanic desert. J. Geophys. Res. 109, C03043. doi:10.1029/2003JC001938.

Barth, A., Alvera-Azcárate, A., Weisberg, R.H., 2008a. A nested model study of the Loop Current generated variability and its impact on the West Florida Shelf. J. Geophys. Res. 113, C05009. doi:10.1029/2007JC004492.

Barth, A., Alvera-Azcárate, A., Weisberg, R.H., 2008b. Assimilation of high-frequency radar currents in a nested model of the West Florida Shelf. J. Geophys. Res. 113, C08033. doi:10.1029/2007JC004585.

Barth, A., Alvera-Azcárate, A., Weisberg, R.H., 2008c. Benefit of nesting a regional model into a large-scale ocean model instead of climatology. Application to the West Florida Shelf. Continental Shelf Res. 28, 561–573.

Bleck, R., Sun, S., Halliwell, G., 2001. Boundary conditions in HYCOM. Manuscript available at: http://hycom.rsmas.miami.edu/hycom-model/doc/boundary.pdf.

Bleck, R., 2002. An oceanic general circulation model framed in hybrid isopycnic-cartesian coordinates. Ocean Modell. 37, 55–88.

Bleck, R., Benjamin, S.G., 1993. Regional weather prediction with a model combining terrain-following and isentropic coordinates. Part 1: model description. Mon. Weather Rev 121, 1770–1785.

Castro, R., Mascareñas, A.S., Durazo, R., Collins, C.A., 2000. Seasonal variation of the salinity and temperature at the entrance of the Gulf of California, Mexico. Ciencias Marinas 26 (4), 561–583.

Castro, R., Durazo, R., Mascareñas, A., Collins, C.A., Trasviña, A., 2006. Thermohaline variability and geostrophic circulation in the southern portion of the Gulf of California. Deep-Sea Res. I 53, 188–200.

Cheng, W., McPhaden, M.J., Zhang, D., Metzger, E.J., 2007. Recent changes in the pacific subtropical cells inferred from an eddy-resolving ocean circulation model. J. Phys. Oceanogr. 37, 1340–1356.

Christensen Jr., N., de la Paz, R., Gutierrez, G., 1983. A study of sub-inertial waves off the west coast of Mexico. Deep-Sea Res. 30, 835–850.

Csanady, G.T., 1977. Intermittent 'Full' Upwelling in Lake Ontario. J. Geophys. Res. 82, 397–419.

Enfield, D.B., Allen, J.S., 1983. The generation and propagation of sea level variability along the Pacific coast of Mexico. J. Phys. Oceanogr. 13, 1012–1033.

Gierach, M.M., Subrahmanyam, B., 2008. Biophysical responses of the upper ocean to major Gulf of Mexico hurricanes in 2005. J. Geophys. Res. 113, C04029. doi:10.1029/2007JC004419.

Gierach, M.M., Subrahmanyam, B., Thoppil, P.G., 2009. Physical and biological responses to Hurricane Katrina (2005) in a 1/25 nested Gulf of Mexico HYCOM. J. Maine Syst. 78. doi:10.1016/j.jmarsys.2009.05.002, 168-179.

Gill, A.E., 1984. On the behaviour of internal waves in the wake of storms. J. Phys. Oceanogr. 14, 1129–1151.

Gjevik, B., Merrifield, M.A., 1993. Shelf sea response to tropical storms along the west coast of Mexico. Contin. Shelf Res. 13, 25–47.

Godínez, V.M., Beir, E., Lavín, M.F., Kurczyn, J.A., in press. Circulation at the entrance of the Gulf of California from satellite altimeter and hydrographic observations. J. Geophys. Res. doi:2009JC005705.

Han, W., Moore, A.M., Levin, J., Zhang, B., Arango, H.G., Curchitser, E., Di Lorenzo, E., Gordon, A.L., Lin, J., 2009. Seasonal surface ocean circulation and dynamics in the Philippine Archipelago region during 2004–2008. Dyn. Atmos. Oceans. 114–137. doi:10.1016/j.dynatmoce.2008.10.007.

Halliwell, G.R., Barth, A., Weisberg, R.H., Hogan, P.J., Smedstad, O.M., Cummings, J., 2009. Impact of GODAE products on nested HYCOM simulations of the West Florida Shelf. Ocean Dyn. 59. doi:10.1007/s10236-008-0173-2.

Hastenrath, S., 1991. Climate Dynamics of the Tropics. Kluwer Academic Publishers, Dordrecht. 488 pp.

Jaimes, B., Shay, L.K., in press. Mixed layer cooling in mesoscale oceanic eddies during Hurricanes Katrina and Rita. Mon. Weather Rev. doi:10.1175/2009MWR2849.1.

Kara, A.B., Wallcraft, A.J., Hurlburt, H.E., 2005a. A new solar radiation penetration scheme for use in ocean mixed layer studies: An application to the Black Sea using a fine resolution HYbrid Coordinate Ocean Model (HYCOM). J. Phys. Oceanogr. 35, 13–32.

Kara, A.B., Wallcraft, A.J., Hurlburt, H.E., 2005b. How does solar attenuation depth affect the ocean mixed layer? Water turbidity and atmospheric forcing impacts on the simulation of seasonal mixed layer variability in the turbid Black Sea. J. Climate 18, 389–409.

Kara, A.B., Wallcraft, A.J., Hurlburt, H.E., 2005c. Sea surface temperature sensitivity to water turbidity from simulations of the turbid Black Sea using HYCOM. J. Phys. Oceanogr. 35, 33–54.

Kara, A.B., Metzger, E.J., Hurlburt, H.E., Wallcraft, A.J., Chassignet, E.P., 2008. Multistatistics metric evaluation of ocean general circulation model sea surface temperature: application to 0.08_ Pacific Hybrid Coordinate Ocean Model simulations. J. Geophys. Res. 113, C12018. doi:10.1029/2008JC004878.

Kelly, K.A., Thompson, L., Cheng, W., Metzger, E.J., 2007. Evaluation of HYCOM in the Kuroshio extension region using new metrics. J. Geophys. Res. 112, C01004. doi:10.1029/2006JC003614.

Keen, T.R., Allen, S., 2000. The Generation of internal Waves on the Continental Shelf by Hurricane Andrew. J. Geophys. Res. 105, C11, 26203–26224.

Kourafalou, V.H., Peng, G., Kang, H., Hogan, P.J., Smedstadt, O.M., Weisberg, R.H., 2009. Evaluation of Global Ocean data assimilation experiment products on South Florida nested simulations with the Hybrid Coordinate Ocean Model. Ocean Dyn. 59, 47–66. doi:10.1007/s10236-008-0160-7.

Martínez, J.A., Allen, J.S., 2004. A modelling study of coastal-trapped wave propagation in the Gulf of California. Part I: response to remote forcing. J. Phys. Oceanogr. 34, 1313–1331.

Merrifield, M.A., 1992. A comparison of long coastal-trapped wave theory with remote-storm-generated wave events in the Gulf of California. J. Phys. Oceanogr. 22, 5–18.

Metzger, E.J., Zamudio, L., Hurlburt, H.E., Hogan, P.J., 2004. A Hurricane Juliette generated coastally trapped wave in the HYbrid Coordinate Ocean Model (HYCOM), Eos Trans. AGU, 84(52), Ocean Sci. Meet, Suppl., Abstract OS21L-06.

Large, W.G., McWilliams, J.C., Doney, S.C., 1994. Oceanic vertical mixing: a review and a model with a nonlocal boundary layer parameterization. Rev. Geophys. 32, 363–403.

López, M., Zamudio, L., Padilla, F., 2005. Effects of the 1997–1998 El Niño on the exchange of the northern Gulf of California. J. Geophys. Res. 110, C11005. doi:10.1029/2004JC002700.

Prasad, T.G., Hogan, P.J., 2007. Upper-ocean response to Hurricane Ivan in a 1/25° nested Gulf of Mexico HYCOM. J. Geophys. Res. 112, C04013. doi:10.1029/2006JC003695.

Rosmond, T.E., Teixeira, J., Peng, M., Hogan, T.F., Pauley, R., 2002. Navy Operational Global Atmospheric Predictions System (NOGAPS): forcing for ocean models. Oceanography 15 (1), 99–108.

Strub, P.T., James, C., 2002. Altimeter-derived surface circulation in the large-scale NE Pacific gyres: Part 2. 1997–1998 El Niño anomalies, Prog. Oceanogr. 185–214.

Zamudio, L., Hurlburt, H.E., Metzger, E.J., Smedstad, O.M., 2002. On the evolution of coastally trapped waves generated by Hurricane Juliette along the Mexican West Coast, Geophys. Res. Lett. 29(23), 2141. doi:10.1029/2002GL014769.

Zamudio, L., Metzger, E.J., Hurlburt, H.E., Hogan, P.J., 2004. On the monthly variability in the Gulf of California, Eos Trans. AGU, 84(52), Ocean Sci. Meet, Suppl., Abstract OS31D-02.

Zamudio, L., Hurlburt, H.E., Metzger, E.J., Tilburg, C., 2007. Tropical wave-induced oceanic eddies at Cabo Corrientes and the María Islands, Mexico. J. Geophys. Res. 112, C05048. doi:10.1029/2006JC004018.

Zamudio, L., Hogan, P.J., 2008. Nesting the Gulf of Mexico in Atlantic HYCOM: Oceanographic Processes Generated by Hurricane Ivan. Ocean Modell. , 21(3–4), 106–125. doi:10.1016/j.ocemod.2007.12.002.

Zamudio, L., Hogan, P.J., Metzger, E.J., 2008. Summer generation of the Southern Gulf of California eddy train. J. Geophys. Res. 113, C06020. doi:10.1029/2007JC004467.